

Figure 1. Optimized geometries (Å; deg) and natural orbital occupancies of **2b(i)**–(iii).

(40–60 °C). These solvolysis experiments are consistent with the formation of a *symmetrical* zwitterionic intermediate **2a**, wherein the two methylene groups are nucleophilic and chemically equivalent. The close similarity of the  $E_a$  of the rearrangement and the methanolysis suggests that both reactions proceed through the same reaction pathway involving the dialkoxy TMM **2a**.<sup>12</sup>

We also generated the methyl-substituted TMMs **6** from MCPs **5**<sup>4b</sup> and studied their stereochemical behavior through methanol trapping and thermal isomerization (Scheme II). Thus, the reaction of **5E**<sup>5b</sup> and **5Z**<sup>5b</sup> in CD<sub>3</sub>OD at 70 °C quantitatively and stereospecifically gave the (*E*)-tiglate (**8E**) and (*Z*)-tiglate ortho esters (**8Z**), respectively.<sup>6</sup> Evidently, the stereospecific ring opening gave TMMs, **6E** and **6Z**, as discrete intermediates. While the methanolysis allowed trapping of each TMM stereoisomer, thermolysis experiments indicated that these isomers undergo stereochemical isomerization. Thus, heating of both **5E** and **5Z** at 100 °C in toluene resulted in clean interconversion of these isomers. This experiment also generated a third isomer, **7**,<sup>5</sup> as the result of an alternative ring closure (Scheme II), and **7** in turn gave **5E** and **5Z** upon heating. The equilibrium ratio (100 °C) of **5E**, **5Z**, and **7** (starting from pure isomer) was 62:30:8.<sup>13</sup>

Ab initio four electron/four orbital CASSCF (three  $\pi$  orbitals of the allylic system and the p orbital of the remaining carbon: 6-31G basis set) calculations were carried out on the singlet state of **2b**<sup>14</sup> to determine the geometry and nature of the intermediate (Figure 1). It has been found that all three possible low-energy conformers, the C<sub>2v</sub>-planar **2b(i)**, the C<sub>2v</sub>-bisected **2b(ii)**, and the C<sub>s</sub>-bisected **2b(iii)** were found to be most stable, and **2b(ii)** and **2b(i)** were found to be only 4.23 and 4.44 kcal/mol higher in energy, respectively.<sup>15</sup> All these conformers should be equally available for the intermolecular reactions, since the energy barriers separating the three rotational isomers must be small.<sup>1a</sup> Although **2b(ii)** and **2b(iii)** are pure diradicals by symmetry, **2b(i)** has some zwitterionic character (Figure 1) and is best described in terms

of the resonance structures **2b(i)**<sub>I</sub> and **2b(i)**<sub>II</sub>. It is reasonable to suggest that the contribution of these two resonance forms should be influenced upon going from the gas to the polar liquid phase and that the reactivity of **2a** toward polar reactants (e.g., methanol) is governed by the zwitterionic character of **2b(i)**. In this case, the allylic moiety of **2a** can be viewed as a four  $\pi$  electron system (**2b(i)**<sub>I</sub>) suitable for undergoing stereospecific [3 + 2] cycloaddition to electron-deficient olefins.<sup>5a</sup>



**Supplementary Material Available:** Preparation of MCPs and the experimental details of their rearrangement and methanolysis (14 pages). Ordering information is given on any current masthead page.

### The First Homoleptic Alkoxide Dimers of Rhenium(V) and Tungsten(V). Stereochemical Consequences of Metal–Metal Bonding in Edge-Shared Biotetrahedra

Jeffrey C. Bryan,<sup>1a</sup> David R. Wheeler,<sup>1a</sup> David L. Clark,<sup>1b</sup> John C. Huffman,<sup>1c</sup> and Alfred P. Sattelberger\*<sup>1d</sup>

*Inorganic and Structural Chemistry Group (INC-4) and Nuclear and Radiochemistry Group (INC-11) Los Alamos National Laboratory Los Alamos, New Mexico 87545 Molecular Structure Center, Indiana University Bloomington, Indiana 47405 Received November 26, 1990*

Edge-shared biotetrahedral transition-metal complexes of general formula M<sub>2</sub>L<sub>10</sub> have long been recognized as one of the four most frequently occurring structural types for dinuclear compounds that contain metal–metal bonds.<sup>2</sup> Such complexes can, in principle, exhibit metal–metal single, double, and triple bonds by overlap of metal d orbitals. While the concept of a triple bond for edge-shared biotetrahedra is enigmatic,<sup>3–5</sup> single and double bonds of valence electronic configuration  $\sigma^2$  and  $\sigma^2\pi^2$  are well-known for d<sup>1</sup> and d<sup>2</sup> early transition metals.<sup>3</sup> An exception to this observation can be found in high-oxidation-state d<sup>1</sup> and d<sup>2</sup> metal halides, M<sub>2</sub>Cl<sub>10</sub> (M = Mo, W, Re), which are paramagnetic with M–M distances on the order of 3.7 Å.<sup>6–8</sup> It has been suggested that replacement of bridging chloride ligands with bridging-oxygen donors may reduce the positive charge on the metal atoms and facilitate d–d overlap in d<sup>1</sup> and d<sup>2</sup> dimers.<sup>9</sup> Here we describe the synthesis and molecular and electronic structures of two new high-oxidation-state edge-shared biotetrahedral complexes, W<sub>2</sub>(OMe)<sub>10</sub> and Re<sub>2</sub>(OMe)<sub>10</sub>, which fulfill this expectation.

The addition of 1 equiv of lithium powder to a THF solution of *cis*-WF<sub>2</sub>(OMe)<sub>4</sub> (prepared from WF<sub>6</sub> and neat Me<sub>3</sub>SiOMe<sup>10</sup>) produces a mixture of red tungsten(V) products characterized as W<sub>2</sub>F<sub>x</sub>(OMe)<sub>10-x</sub> where  $x = 1–3$  based on <sup>1</sup>H and <sup>19</sup>F NMR. This mixture reacts with excess sodium methoxide in THF to form blue W<sub>2</sub>(OMe)<sub>10</sub> (**1**)<sup>11</sup> as the only soluble tungsten product (70% yield,

(12) An unlikely alternative (experimentally distinguishable, however, ref 4a) is that the methanolysis involves a bimolecular addition of a methoxide anion to **1a** to give a symmetrical allylic anion. We thank a referee for reminding us of this possibility.

(13) Interconversion between **5E** and **7** takes place rapidly at 80 °C, while conversion to and from **5Z** requires a week at 100 °C.

(14) (a) For the chemistry and molecular orbitals of dimethoxy TMM incorporated in a five-membered ring, see: Carpenter, B. K.; Little, R. D.; Berson, J. A. *J. Am. Chem. Soc.* **1976**, *98*, 5723. Platz, M. S.; McBride, J. M.; Little, R. D.; Harrison, J. J.; Shaw, A.; Potter, S. E.; Berson, J. A. *J. Am. Chem. Soc.* **1976**, *98*, 5725. Siemionko, R.; Shaw, A.; O'Connell, G.; Little, R. D.; Carpenter, B. K.; Shen, L.; Berson, J. A. *Tetrahedron Lett.* **1978**, 3529. (b) Berson, J. A. *Acc. Chem. Res.* **1978**, *11*, 446.

(15) Presumably, all of these are not local minima, but no confirmation has been made.

(1) (a) INC-4, Mail Stop C345. (b) INC-11, Mail Stop G739. (c) Indiana University. (d) INC-DO, Mail Stop J515.

(2) Cotton, F. A.; Wilkinson, G. *Advanced Inorganic Chemistry*, 5th ed.; Wiley-Interscience: New York, 1988; Chapter 23.

(3) Cotton, F. A. *Polyhedron* **1987**, *6*, 667.

(4) Cotton, F. A.; Diebold, M. P.; O'Connor, C. J.; Powell, G. L. *J. Am. Chem. Soc.* **1985**, *107*, 7438.

(5) Chakravarty, A. R.; Cotton, F. A.; Diebold, M. P.; Lewis, D. B.; Roth, W. J. *J. Am. Chem. Soc.* **1986**, *108*, 971.

(6) Sands, D. E.; Zalkin, A. *Acta Crystallogr.* **1959**, *12*, 723.

(7) Cotton, F. A.; Rice, C. E. *Acta Crystallogr., Sect. B* **1978**, *34*, 2833.

(8) Mucker, K.; Smith, G. S.; Johnson, Q. *Acta Crystallogr., Sect. B* **1968**, *24*, 874.

(9) Anderson, L. B.; Cotton, F. A.; DeMarco, D.; Fang, A.; Ilsley, W. H.; Kolthammer, B. W. S.; Walton, R. A. *J. Am. Chem. Soc.* **1981**, *103*, 5078.

(10) Handy, L. B.; Sharp, K. G.; Brinkman, F. E. *Inorg. Chem.* **1972**, *11*, 523.

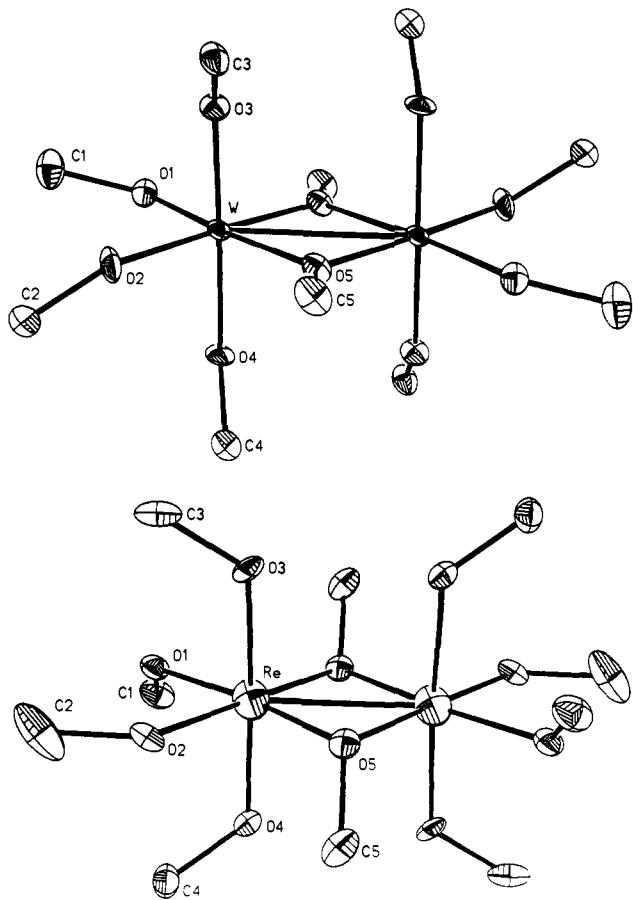
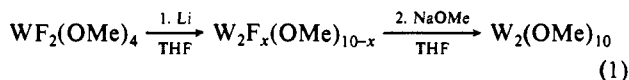
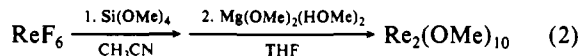


**Figure 1.** ORTEP drawings of  $W_2(OMe)_{10}$  (top) and  $Re_2(OMe)_{10}$  (bottom) emphasizing the orientation of the axial alkoxide ligands relative to the metal-metal bond. Important bond distances (Å) and angles (deg) for **1**:  $W-W = 2.7897$  (8),  $W-O(2) = 1.963$  (6),  $W-O(4) = 1.887$  (6),  $W-O(5) = 2.028$  (6),  $W-O(5)-W = 85.6$  (2),  $W-O(2)-C(2) = 128.2$  (6),  $W-O(4)-C(4) = 135.1$  (6), and  $O(3)-W-O(4) = 169.8$  (3). For **2**:  $Re-Re = 2.5319$  (7),  $Re-O(2) = 1.943$  (4),  $Re-O(4) = 1.907$  (4),  $Re-O(5) = 2.036$  (4),  $Re-O(5)-Re = 76.44$  (16),  $Re-O(2)-C(2) = 125.6$  (4),  $Re-O(4)-C(4) = 124.9$  (4), and  $O(3)-Re-O(4) = 176.7$  (2).

eq 1). Air-sensitive **1** is the first reported example of a homoleptic tungsten(V) alkoxide, although mixed chloro-alkoxy tungsten(V) dimers are known.<sup>12,13</sup>



Condensation of  $ReF_6$  into an acetonitrile solution of  $Si(OMe)_4$  at  $-40^\circ C$  followed by slow warming to room temperature produces a mixture of products,<sup>14</sup> including  $Re_2(OMe)_{10}$  (**2**).<sup>11</sup> The isolated mixture reacts with excess  $Mg(OMe)_2(HOME)_2$  in THF solution to give red **2** as the only isolable rhenium product ( $\sim 60\%$  based on  $ReF_6$ , eq 2). Air-sensitive **2** is the first example of a rhenium(V) alkoxide.



Compounds **1** and **2** are soluble and stable in most common organic solvents at  $25^\circ C$ . Room temperature  $^1H$  NMR spectra

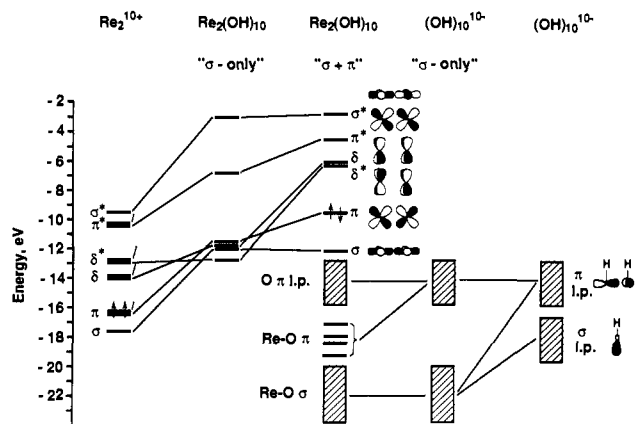


**Figure 2.** Results of Fenske-Hall calculations on  $Re_2(OH)_{10}$  under  $D_{2h}$  symmetry. This diagram shows the effects of metal-oxygen  $\sigma$ -bonding in the column labeled " $\sigma$ -only" and the effects of the  $\pi$  lone-pair interactions in the column labeled " $\sigma + \pi$ ". The results for  $W_2(OH)_{10}$  were similar with the M-M  $\sigma$ -bonding orbital as the HOMO.

( $C_6D_6$ ) for both **1** and **2** exhibit three sharp singlets in a 2:2:1 ratio consistent with an edge-shared bioctahedral geometry.<sup>11</sup> Single-crystal X-ray structural data confirm the expected edge-shared bioctahedral geometries (Figure 1) and reveal metal-metal distances of 2.7897 (8) Å (W) and 2.5319 (7) Å (Re) indicative of metal-metal single and double bonds, respectively.<sup>11</sup> The axial alkoxide ligands have short average M-O distances ( $W-O = 1.88$  Å,  $Re-O = 1.90$  Å)<sup>15</sup> compared to the average equatorial M-O distances ( $W-O = 1.94$  Å,  $Re-O = 1.95$  Å). Both observations prompted an investigation of the electronic structure of  $M_2(OH)_{10}$  models using the method of Fenske and Hall.<sup>16,17</sup>

The interaction of the OH ligand set with the valence orbitals of the  $M_2$  manifold is most easily visualized in terms of spatially and energetically inequivalent  $\sigma$  and  $\pi$  lone-pair orbitals of the free OH ligand, derived from an  $sp$ -hybridized oxygen atom. These important ligand orbitals are depicted qualitatively on the right of Figure 2. Using the "frozen  $\pi$  orbital" approximation,<sup>18,19</sup> interaction of the set of  $(OH)_{10}^{10-}$   $\sigma$  lone pairs with the well-known<sup>20</sup>  $M_2^{10+}$  fragment orbitals results in a large splitting of the  $M_2$  core orbitals as a consequence of M-O  $\sigma$ -bonding as seen in Figure 2 for  $M = Re$ . One orbital of each degenerate set of  $M_2^{10+}$   $\pi$ ,  $\delta$ ,  $\delta^*$ , and  $\pi^*$  orbitals is removed from the M-M bonding manifold because of strong M-O  $\sigma$ -bonding which occurs at lower energy. The destabilization of the M-M  $\sigma$ ,  $\pi$ ,  $\delta$ ,  $\pi^*$ , and  $\sigma^*$  orbitals is a consequence of "through-bond coupling" as described by Hoffmann.<sup>21</sup> The  $\sigma$ -only bonding picture yields a ground-state electronic configuration of  $\delta^{*2}\sigma^2$  (Re) with a nearly isoenergetic HOMO and LUMO, similar to that observed for  $Re_2Cl_{10}$ .<sup>21</sup> In the central column of Figure 2 the  $\pi$ -bonding interactions have been switched on and the effects of  $\pi$ -bonding on orbital energetics can be rationalized from simple perturbation theory. The alkoxide  $\pi$ -interaction takes place only with  $M_2$  core orbitals of  $\pi$  and  $\delta$  symmetry with the largest  $\pi$ -interaction between  $M_2$   $\delta$  and  $\delta^*$  orbitals. This  $\pi$ -bonding interaction removes the  $\delta$  and  $\delta^*$  orbitals from the valence region, generates a sizable HOMO-LUMO gap,

(15) (a) Chisholm, M. H. *Polyhedron* **1983**, *2*, 681. (b) Chisholm, M. H.; Clark, D. L. *Comments Inorg. Chem.* **1987**, *6*, 23.

(16) Hall, M. B.; Fenske, R. F. *Inorg. Chem.* **1972**, *11*, 768.

(17) (a) Bursten, B. E.; Jensen, J. R.; Fenske, R. F. *J. Chem. Phys.* **1978**, *68*, 3320. (b) Hehre, W. J.; Stewart, R. F.; Pople, J. A. *J. Chem. Phys.* **1969**, *51*, 2657.

(18) Cayton, R. H.; Chisholm, M. H.; Clark, D. L.; Hammond, C. E. *J. Am. Chem. Soc.* **1989**, *111*, 2751.

(19) (a) Roothaan, C. C. *J. Rev. Mod. Phys.* **1951**, *23*, 69. (b) Lichtenberger, D. L.; Fenske, R. F. *J. Chem. Phys.* **1976**, *64*, 4247.

(20) (a) Norman, J. G., Jr.; Kolari, H. J.; Gray, H. B.; Troglor, W. C. *Inorg. Chem.* **1977**, *16*, 987. (b) Bursten, B. E.; Cotton, F. A. *Faraday Symp. Chem. Soc.* **1980**, No. 14, 180.

(21) Shaik, S.; Hoffmann, R.; Fisel, C. R.; Summerville, R. H. *J. Am. Chem. Soc.* **1980**, *102*, 4555.

(11) Analytical, spectroscopic, and crystallographic data are supplied as supplementary material.

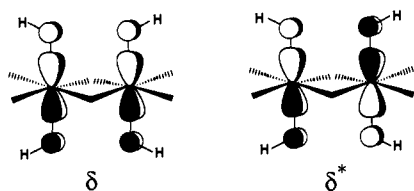
(12) Cotton, F. A.; DeMarco, D.; Kolthammer, B. W. S.; Walton, R. A. *Inorg. Chem.* **1981**, *20*, 3048.

(13) Barder, T. J.; Cotton, F. A.; Lewis, D.; Schwotzer, W.; Tetrick, S. M.; Walton, R. A. *J. Am. Chem. Soc.* **1984**, *106*, 2882.

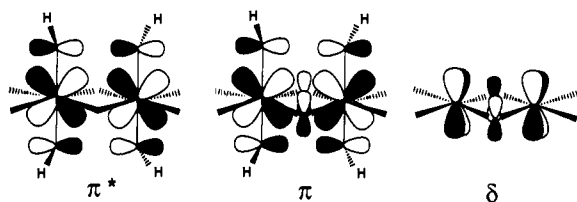
(14) (a)  $Re(OMe)_6$  is obtained (80% yield) when  $ReF_6$  is cocondensed with  $Si(OMe)_4$  at  $-196^\circ C$ , followed by slow warming to room temperature.<sup>12b</sup> (b) Jacob, E. *Angew. Chem., Int. Ed. Engl.* **1982**, *21*, 142.

and yields a diamagnetic  $\sigma^2\pi^2$  double bond for  $M = \text{Re}$ . The calculations for  $M = \text{W}$  yield a similar MO diagram with two fewer electrons and a  $\sigma^2$  ground-state electronic configuration.

Based on conventional electron counting procedures, each Re atom in  $\text{Re}_2(\text{OMe})_{10}$  has 16 valence electrons in the absence of M-O  $\pi$ -bonding. Since the M-M  $\sigma$  and  $\pi$  orbitals are occupied by metal d electrons, this leaves the metal  $\delta$  and  $\delta^*$  orbitals available for  $\pi$ -bonding interactions. The alkoxide ligand can only form  $\pi$ -bonds with M-M  $\delta$ -type orbitals by alignment parallel to the metal-metal axis as observed in the crystal structure of  $\text{Re}_2(\text{OMe})_{10}$ . The four  $\pi$  electrons donated into the M-M  $\delta$  and  $\delta^*$  orbitals bring each Re atom to an 18-valence-electron count. These important  $\pi$ -bonding interactions are illustrated schematically below.



In  $\text{W}_2(\text{OMe})_{10}$ , each W atom has 14 valence electrons in the absence of M-O  $\pi$ -bonding, and only the M-M  $\sigma$ -bonding orbital is occupied by metal electrons. This leaves the M-M  $\pi$ ,  $\delta$ ,  $\delta^*$ , and  $\pi^*$  orbitals available for M-O  $\pi$ -bonding. In order for the alkoxides to engage in maximum  $\pi$ -bonding, the bridging ligands rehybridize to planar  $sp^2$ , making the  $\pi$  lone pairs available for  $\pi$ -bonding interactions in the bridge. The bridging ligands can only interact by symmetry with the bonding M-M  $\pi$  and  $\delta$  orbitals; the interaction is found to be strongest with the  $\delta$  orbitals. To avoid a competition between bridge and axial ligand  $\pi$ -bonding with  $\delta$  orbitals, the axial ligands rotate  $90^\circ$  to form equally strong  $\pi$ -bonds with M-M  $\pi$  and  $\pi^*$  orbitals (Figure 1). The six electrons donated from oxygen  $\pi$  lone pairs into M-M  $\pi$ ,  $\pi^*$ , and  $\delta$  orbitals bring each W atom to 17 valence electrons ( $34 e^-/\text{dimer}$ ). These  $\pi$ -bonding interactions are illustrated schematically below.



Combined with the known  $\text{Ta}_2(\text{OMe})_{10}$ ,<sup>22</sup> a fundamental series of third-row decamethoxide dimers has been realized spanning  $d^0-d^0$ ,  $d^1-d^1$ , and  $d^2-d^2$ . Full details of the synthetic chemistry, physicochemical properties, and electronic structure calculations will be presented in future publications.<sup>23-25</sup>

**Acknowledgment.** This work was performed under the auspices of the Division of Chemical Energy Sciences, Office of Energy Sciences, Office of Energy Research, U.S. Department of Energy; financial support is gratefully acknowledged. We also thank Professors B. E. Bursten, M. H. Chisholm, and D. L. Lichtenberger for helpful discussions.

(22) (a) Bradley, D. C.; Wardlaw, W.; Whitley, A. *J. Chem. Soc.* **1955**, 726. (b) Riess, J. G.; Hubert-Pfalzgraf, L. G. *Chimia* **1976**, *30*, 481. (c) Pinkerton, A. A.; Schwarzenbach, D.; Hubert-Pfalzgraf, L. G.; Riess, J. G. *Inorg. Chem.* **1976**, *15*, 1196. (d) The X-ray structure of  $\text{Ta}_2(\text{OMe})_{10}$  is currently under investigation.

(23) Bryan, J. C.; Wheeler, D. R.; Clark, D. L.; Huffman, J. C.; Sattelberger, A. P., in preparation.

(24) Wheeler, D. R.; Bryan, J. C.; Jatcko, M.; Lichtenberger, D. L.; Sattelberger, A. P., in preparation.

(25) Bryan, J. C.; Wheeler, D. R.; Jatcko, M.; Schneider, W. F.; Bursten, B. E.; Lichtenberger, D. L.; Sattelberger, A. P., in preparation.

**Supplementary Material Available:** Analytical, spectroscopic, and crystallographic data for **1** and **2** including tables of atomic coordinates, bond distances and angles, and anisotropic thermal parameters (7 pages); listing of observed and calculated structure factors for **1** and **2** (6 pages). Ordering information is given on any current masthead page.

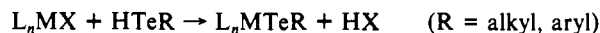
### $(\text{Me}_3\text{Si})_3\text{SiTeH}$ : Preparation, Characterization, and Synthetic Utility of a Remarkably Stable Tellurol

Bashir O. Dabbousi, Philip J. Bonasia, and John Arnold\*

Department of Chemistry, University of California  
Berkeley, California 94720

Received December 24, 1990

Synthetic routes to metal tellurolates, the tellurium analogues of alkoxides and thiolates, are limited.<sup>1</sup> Interest in these compounds heightened recently following reports that materials such as the oligomeric benzenetellurolates  $[\text{M}(\text{TePh})_2]_n$  ( $M = \text{Hg}, \text{Cd}$ ) may serve as precursors to semiconducting bulk metal tellurides  $\text{HgTe}$  and  $\text{CdTe}$ .<sup>2</sup> We are developing tellurolate chemistry supported by large, sterically encumbered ligands in attempts to synthesize atypical metal tellurolates featuring low molecularity and hydrocarbon solubility.<sup>3</sup> At present, the only general route to these compounds involves a metathesis reaction between an alkali-metal tellurolate and a metal halide.<sup>4</sup> Disadvantages include the following: (i) one is limited by the choice of metal halide starting materials; (ii) tellurolate anions are quite reducing; and (iii) the presence of strong donor molecules (either as solvent or ligated to the tellurolate salts) often interferes with product purification. In searching for more versatile routes, we considered the following tellurolysis pathway:



Analogous reactivity is well-documented for alcohols,<sup>5</sup> thiols,<sup>6</sup> and selenols,<sup>7</sup> where reactions are extremely flexible with respect to the choice of R and the leaving group X (e.g., X = alkyl, amide, alkoxide, etc.); in addition, these reactions are best carried out in nonpolar solvents. For tellurolysis, however, a major drawback has been that known tellurols are thermally unstable compounds that are difficult to isolate and purify.<sup>8-11</sup>

(1) Gysling, H. J. In *The Chemistry of Organic Selenium and Tellurium Compounds*; Patai, S., Rappoport, Z., Eds.; Wiley: New York, 1986; Vol. 1, p 679. Gysling, H. J. *Coord. Chem. Rev.* **1982**, *42*, 133.

(2) Brennan, J. G.; Siegrist, T.; Carroll, P. J.; Stuczynski, S. M.; Reynnders, P.; Brus, L. E.; Steigerwald, M. L. *Chem. Mater.* **1990**, *2*, 403. Stuczynski, S. M.; Brennan, J. G.; Steigerwald, M. L. *Inorg. Chem.* **1989**, *28*, 4431. Brennan, J. G.; Siegrist, T.; Stuczynski, S. M.; Steigerwald, M. L. *J. Am. Chem. Soc.* **1989**, *111*, 9240. Steigerwald, M. L.; Sprinkle, C. R. *Organometallics* **1988**, *7*, 245. Steigerwald, M. L.; Sprinkle, C. R. *J. Am. Chem. Soc.* **1987**, *109*, 7200.

(3) Bonasia, P. J.; Arnold, J. J. *Chem. Soc., Chem. Commun.* **1990**, 1299.

(4) For examples, see: Gardner, S. A. *J. Organomet. Chem.* **1980**, *190*, 289. Davies, I.; McWhinnie, W. R. *J. Inorg. Nucl. Chem. Lett.* **1976**, *12*, 763 and ref 1 for reviews.

(5) Bradley, D. C.; Mehrotra, R. C.; Gaur, D. P. *Metal Alkoxides*; Academic: New York, 1978. Rothwell, I. P. R.; Chisholm, M. H. In *Comprehensive Coordination Chemistry*; Wilkinson, G., Gillard, R. D., McCleverty, J. A., Eds.; Pergamon: New York, 1987; Vol. 2, p 335. Caulton, K. G.; Hubert-Pfalzgraf, L. G. *Chem. Rev.* **1990**, *90*, 969.

(6) Dance, I. G. *Polyhedron* **1986**, *5*, 1037. Blower, P. G.; Dilworth, J. R. *Coord. Chem. Rev.* **1987**, *76*, 121. Vyazankin, N. S.; Bochkarev, M. N.; Charov, A. I. *J. Organomet. Chem.* **1971**, *27*, 175.

(7) For example: Bochmann, M.; Webb, K.; Harman, M.; Hursthouse, M. B. *Angew. Chem., Int. Ed. Engl.* **1990**, *29*, 638.

(8) In situ generated tellurols are useful synthetic reagents. For reactions involving addition of  $\text{HTeR}$  across  $\text{C}\equiv\text{C}$  bonds in acetylenes, see: Barros, S. M.; Dabdoub, M. J.; Dabdoub, V. M. B.; Comassetto, J. V. *Organometallics* **1989**, *8*, 1661 and references therein. Reviews of organotellurium reagents in organic synthesis: Engman, L. *Phosphorus Sulfur Relat. Elem.* **1988**, *38*, 105. Petraghani, N.; Comassetto, J. V. *Synthesis* **1986**, 1.